Minerals Engineering 56 (2014) 112–120

Contents lists available at ScienceDirect

Minerals Engineering

journal homepage: www.elsevier.com/locate/mineng

Characterisation and liberation of chromium from fine ferrochrome waste materials

Y. van Staden [a], J.P. Beukes [a,*], P.G. van Zyl [a], J.S. du Toit [b], N.F. Dawson [a,c]

[a] Chemical Resource Beneficiation, North-West University, Potchefstroom Campus, Private Bag X6001, Potchefstroom 2520, South Africa
[b] ASA Metals (Pty) Ltd., PO Box 169, Burgersfort 1150, South Africa
[c] Glencore Alloys, PO Box 2131, Rustenburg 0300, South Africa

ARTICLE INFO

Article history:
Received 7 August 2013
Accepted 5 November 2013
Available online 1 December 2013

Keywords:
Cr liberation
Ferrochrome waste
Aqueous ozonation
Ozone (O_3)
Advanced oxidation process

ABSTRACT

Three types of generic chromium (Cr)-containing wastes are generated during ferrochrome (FeCr) production, i.e. slag, bag filter dust (BFD) and venturi sludge. Slag is by volume the largest waste; however, fine FeCr waste materials (e.g. BFD, venturi sludge) are from an environmental perspective the most important. The loss of Cr units to FeCr waste streams represents both an added cost burden (related to disposal/storage) and a loss of revenue in terms of contained Cr units. In this paper, the novel idea of the liberation of Cr units from FeCr BFD and the ultra-fine fraction of slag (UFS) with aqueous ozonation and the advanced oxidation process was investigated. Several techniques were used to characterise both case study waste materials, i.e. particle size distribution, chemical composition, chemical surface composition and crystalline content analysis. Results indicated that limited Cr liberation could be obtained from the waste materials utilising aqueous ozonation. For BFD, only a maximum of 4.2% of total Cr liberation was achieved. However, the Cr liberation of BFD was substantially higher than that achieved for the UFS, which was attributed to the difference in characteristics of the two materials. Cr liberation observed was related to the formation of the $OH^{\cdot}$ radicals during the spontaneous decomposition of aqueous O_3. Application of the advanced oxidation process by the addition of H_2O_2 during ozonation increased Cr liberation dramatically. More than 21% of total Cr liberation could be achieved for both the waste materials used in this investigation. Although the afore-mentioned Cr liberation level is unlikely to be commercially viable, the investigation proved that further research could optimise this process.

1. Introduction

Chromium (Cr) is an essential element in modern-day society. The only commercially recoverable source of Cr is chromite (Murthy et al., 2011; Riekkola-Vanhanen, 1999). Approximately 90% of all mined chromite is used in the manufacturing of ferrochrome (FeCr) (Rao, 2010), which is mostly produced by the carbothermic reduction of chromite (Riekkola-Vanhanen, 1999). Various grades of FeCr can be produced, with high carbon FeCr being the most common. FeCr is mainly used in the production of stainless steel (Murthy et al., 2011), of which the application and demand are growing at a significant rate (ISSF, 2011).

South Africa holds approximately three quarters of the world's viable chromite reserves (Cramer et al., 2004) and, in 2009, produced approximately 39% of the global annual high carbon FeCr (ICDA, 2010). Beukes et al. (2010) presented an overview of the processes utilised by the South African FeCr industry. Although this review (Beukes et al., 2010) referred specifically to the South African FeCr industry, similar processes are also applied internationally. According to this review, FeCr is currently mainly produced with (i) conventional semi-closed/open submerged arc furnace (SAF) operation, with bag filter off-gas treatment; (ii) closed SAF operation that usually utilises oxidative sintered pelletised feed, with venturi scrubbing of off-gas; (iii) closed SAF operation consuming pre-reduced pelletised feed, with venturi scrubbing of off-gas; and (iv) closed direct current (DC) arc furnace operation, with venturi scrubbing of off-gas.

Three types of generic Cr-containing wastes are generated during FeCr production utilising the afore-mentioned FeCr production processes. Slag is generated during the smelting process, bag filter dust (BFD) during the cleaning of the off-gas originating from semi-closed/open furnaces, and venturi sludge during the scrubbing of the off-gas from closed furnaces. Although slag is by volume the largest waste produced during FeCr production, BFD is environmentally considered to be the most important waste, since it

* Corresponding author. Tel.: +27 82 460 0594; fax: +27 18 299 2350.
E-mail address: paul.beukes@nwu.ac.za (J.P. Beukes).

0892-6875
http://dx.doi.org/10.1016/j.mineng.2013.11.004

contains small amounts of Cr(VI) (Beukes et al, 2010). Venturi sludge is generated in similar volumes than BFD, but contains significantly smaller amounts of Cr(VI) (Beukes et al., 2010; Gericke, 1995). Cr(VI) is generally regarded as carcinogenic, although not all forms of Cr(VI) have been proven to be carcinogenic (IARC, 1997). Beukes et al. (2012) provided an overview of the Cr(VI) treatment strategies currently applied by South African FeCr producers.

Typical Cr recovery during FeCr smelting is 70–93%, depending on the specific smelting technology applied (Naiker and Riley, 2006; Cramer et al., 2004). Due to increased cost, efficiency and environmental pressures, all FeCr producers strive towards reduced waste generation with associated lower Cr unit losses. The loss of Cr units in FeCr production wastes, i.e. slag, BFD and venturi sludge, is a significant contributor to loss of revenue.

The recovery of Cr units from FeCr wastes has up to now mainly been associated with physical separation methods, such as jigging, magnetic separation, dense media separation (DMS), flotation, shaking tables and spirals (e.g. Sripriya and Murty, 2004; Shen and Forssberg, 2002; Coetzer et al., 1997; Visser and Barret, 1992). These processes have also predominantly been limited to the recovery of >75 μm particles, with waste streams consisting of smaller particles being somewhat neglected.

Van der Merwe et al. (2012) indicated that aqueous ozonation could be used to convert water insoluble Cr(III) to soluble Cr(VI). These authors only focused on the possible health and environmental impacts associated with such conversion during water treatment. Additionally, Rodman et al. (2006) indicated that the conversion of Cr(III) propionate to Cr(VI) by the advanced oxidation process could be used as a means of pre-treatment for an analytical technique. The advanced oxidation processes are based on the generation of radical intermediates (usually $OH^{\cdot}$ radicals) to enhance regular oxidation techniques (Neyens and Bayens, 2003; Andreozzi et al, 1999). There are many different variations of the advanced oxidation process. Popular examples of this process include the combination of hydrogen peroxide (H_2O_2) with Fe^{2+} and H_2O_2 in combination with ozone and/or UV (Cortez et al., 2011; Wu et al., 2004). From the studies presented by Van der Merwe et al. (2012) and Rodman et al. (2006), it seems possible that the conversion of insoluble Cr(III) to soluble Cr(VI) could be considered as an alternative method for Cr recovery from wastes. Although this route for Cr recovery seems counterintuitive, since Cr(VI) is generally considered to be carcinogenic, the risks associated with aqueous Cr(VI) is certainly much less than airborne Cr(VI) and these risks can be mitigated (Beukes et al., 2010). Therefore, the possible recovery of Cr units from BFD and the ultra-fine slag fraction (UFS) with aqueous ozonation and the advanced oxidation process was considered in this study.

2. Materials and methods

2.1. Materials

In this paper, two case study waste materials were used, i.e. BFD and the UFS. Both these materials were sampled at one of the large FeCr smelters in South Africa. The BFD was obtained from the bag filter of a semi-closed furnace at this smelter. The UFS originated from the <1 mm circuit at the metal recovery plant, where slags from both semi-closed and closed furnaces of this specific FeCr producer were treated. At the metal recovery plant, the 1–8 and the 8–20 mm slag fractions were treated in air-pulsed jigs to recover the FeCr in these two size fractions. Numerous papers have described similar FeCr recovery systems (Sripriya and Murty, 2004; Visser and Barret, 1992). The <1 mm slag fraction was treated in spirals to recover the liberated FeCr, unaltered chromite and partially altered chromite, which was fed back to the pelletising section at this specific FeCr producer and smelted again. However, before the <1 mm slag fraction was treated in the spirals, the ultra-fine fraction was removed with a cyclone (cyclone overflow). This ultra-fine fraction was then dewatered with a filter press to form a filter cake. This filter cake was sampled from its stockpile and used as the case study UFS.

SARM 8, supplied by Industrial Analytical (Pty) Ltd., was used as a reference material in the determination of total Cr. A reference standard containing 1009 ± 2 μg/mL chromate (CrO_4^{2-}), obtained from Spectrascan, was used to prepare standard solutions to construct a calibration line for Cr(VI) analysis. Sodium hydroxide (NaOH) (Merck) and 98% sulphuric acid (H_2SO_4) (Sigma–Aldrich) were used to adjust the pH. All other chemicals used were of analytical grade (AR). These were received from various suppliers and used without further purification or treatment. In all experiments requiring water, ultra-pure water (resistivity 18.2 MΩ cm^{-1}) was used, which was produced by a Milli-Q water purification system. The medical grade oxygen (O_2) that was used for ozone (O_3) production was supplied by Afrox.

2.2. Case study waste characterisation

The particle size distributions of the case study waste materials were determined by utilising laser diffraction particle sizing (Saturn DigiSizer II 5205). A diluted suspension of each material was ultra-sonicated for 60 s prior to the measurement, in order to disperse the particles and to avoid the use of a chemical dispersant.

A Spectro Ciros vision inductively coupled plasma optical emission spectrometry (ICP–OES) was used to determine the majority of elements present in the two case study materials. The materials were digested prior to ICP–OES analysis with hydrofluoric acid (HF), perchlorate ($HClO_4$) and nitric acid (HNO_3). Thereafter, the solution was made up to the required volume with hydrochloric acid (HCl). The elemental carbon (C) and sulphur (S) contents of the two case study materials were determined by means of combustion and infrared (IR) spectrophotometry utilising a LECO CS 200 and an Eltra CS 2000. A 1:1 mixture of tungsten (W) and iron (Fe) chips was used as the accelerator flux. The phosphor (P) content was determined by dissolution of the case study material in concentrated HNO_3 and $HClO_4$, followed by P complexation with a metavanadate/molybdate colouring agent. The P was then determined colourimetrically in a UV–visible instrument (SHIMADZU 400). Atomic absorption spectroscopy (AAS) was conducted with a Varian spectra 10 to determine the Na content. The materials were prepared for AAS analysis by digestion in HNO_3 and $HClO_4$, where after the solution was made up to the required volume with HCl.

X-ray diffraction (XRD) using a Röntgen diffraction system (PW3040/60 X'Pert Pro) and a back loading preparation method was used to determine the crystalline phases present in the case study FeCr waste materials. The samples were scanned using X-rays generated by a copper (Cu) Kα X-ray tube. The measurements were carried out between variable divergence- and fixed-receiving slits. The phases were identified using X'PertHighscore plus software. The relative phase amounts were estimated using the Rietveld method (Autoquan programme). A limitation of the method applied was that ferrochrome metal was not detected as crystalline phases. In addition, X-ray florescence (XRF) was used to determine the concentration of elements present in the case study materials. The same instrument was used, but a rhodium (Rh) X-ray tube was used to irradiate the samples and a Super Q database was used to determine the multi-elemental concentrations.

Surface analysis of the two case study materials was performed with an FEI Quanta 200 scanning electron microscope (SEM) with an integrated Oxford Instruments INCA 200 energy dispersive

X-ray spectroscopy (EDS) microanalysis system. SEM micrographs were taken at various magnifications to characterise the physical attributes of the two case study materials. SEM–EDS was used to conduct chemical analysis of the surface of the samples. In order to mitigate the negative impact of surface roughness and porosity on SEM–EDS analysis, the area considered during an analysis was moved to cover almost the entire area of the button covered with the material analysed. Such analysis of almost the entire sample button area was referred to as "entire surface" analysis in the results. Additionally no samples were coated with carbon prior to SEM–EDS analysis. However, after the EDS analyses were completed, the same sample buttons were coated with carbon in order to facilitate better micrographs.

2.3. Experimental procedures for chromium liberation

2.3.1. Ozonation experimental procedure

O_3 was produced using a P-HP 250 Sterizone ozone generator. O_2 feed at a flow of 500 NL/h was maintained throughout all experiments. The gaseous O_3 concentration was determined with a Cary 50 Conc UV–visible spectrophotometer. The absorption of O_3 was measured at a wavelength of 254 nm and an absorption coefficient of 3024 L cm^{-1} mol^{-1} was used in the calculation of the gaseous O_3 concentrations (McElroy et al., 1997; Dohan and Masschelein, 1987).

A predetermined mass of the case study material, i.e. BFD or UFS, was suspended in 150 ml of pH-adjusted water. O_3 was bubbled through the solution with a bubble diffuser for a pre-selected ozonation contact time. The particles were kept in suspension by means of continuous stirring with a magnetic stirrer. The sealed glass beaker containing the particle suspension was placed in a water jacket in which the water temperature was controlled. The experimental set-up is similar to that used by Van der Merwe et al. (2012). This experimental setup enabled the monovariance investigation of the influence of different process controlling parameters, e.g. pH, ozonation contact time, waste material solid loading, gaseous O_3 concentration and temperature, on the liberation of Cr from the waste materials.

After each ozonation experiment, the 150 ml Cr(VI)-containing solution was filtered off by means of milli-pore filtering (0.45 μm). The remaining solid residue was washed with 50 ml pH-adjusted water, with the pH correlating to the pH of the specific experiment conducted. The combined solution (filtrate and wash water) was then adjusted to a pH of 12.6 (see Section 2.3.3), transferred to a 250 ml volumetric flask and filled to the mark with water adjusted to a pH of 12.6. The Cr(VI) content of this solution was then determined with the method described in Section 2.3.3. Blank experiments, during which all reaction conditions were kept the same with the O_3 generator switched off, were also performed.

2.3.2. Advanced oxidation process experimental procedure

In the advanced oxidation process, a peroxide and/or ultraviolet (UV) irradiation can be used in conjunction with O_3 to increase the oxidation potential (Bragg et al., 2012; Rodman et al., 2006). In this study, H_2O_2, combined with aqueous ozonation, was used. The experimental procedure was the same as discussed for ozonation (Section 2.3.1), with the exception that H_2O_2 was also added. The fraction of H_2O_2 added, as a fraction of the total aqueous solution ozonated, was varied between 3.3 and 20 vol.%. H_2O_2 was added either at the beginning of the experiment only, or throughout the duration of ozonation contact time.

2.3.3. Cr liberation determinations

In order to calculate the liberation of Cr from the waste materials, the total Cr content of the initial material and Cr(VI) content of the aqueous solution after treatment with ozonation (Section 2.3.1) or the advanced oxidation process (Section 2.3.2) had to be determined.

Total Cr content present was determined by converting all Cr, irrespective of the oxidation state, to water-soluble Cr(VI) (Vogel, 1978). Approximately 2 g of sodium peroxide (Na_2O_2) and 0.5 g of sodium carbonate (Na_2CO_3) were weighed into a zirconium (Zr) crucible. Approximately 0.2 g of the sample was also accurately weighed into the crucible. The materials were then thoroughly mixed. Thereafter, the crucible was fused over a Bunsen flame and swirled continuously until the entire mixture melted. After cooling, the fusion was tapped loose from the crucible and transferred to a 500 ml beaker, where 80 ml of distilled water was added. The solution was then filtered using milli-pore filtering (0.45 μm) in order to separate the Cr(VI) solution from the insoluble fraction. The pH of the above-mentioned Cr(VI) aliquot was measured prior to determining the Cr(VI) content and found to be approximately 12.6. The pH was measured using a Hanna Instrument (HI) 2211 pH/ORP meter with an HI 1131B pH electrode and an HI 7662 temperature probe. The Cr(VI) content in the aliquot was quantified using a Pharmacia Biotech Ultrospec 3 000 UV–visible spectrophotometer with a 10 cm quartz cell. Since the UV–visible spectra of Cr(VI) solutions are pH sensitive, the pH of all the standard solutions was 12.6. A five-point calibration curve for Cr(VI) was determined at 350 nm with concentrations ranging from 200 to 4500 pbb.

In order to verify the accuracy and to determine the precision of the above-mentioned method to determine total Cr content, a certified SARM 8 chromite ore reference material was analysed. The average percentage Cr_2O_3 content with an associated confidence interval of the reference material was certified as 48.9 ± 0.1%. Applying the experimental method used to determine the total Cr-content described above on the reference material and performing six analyses yielded a Cr_2O_3 content of 49 ± 0.8%.

The percentages Cr liberated from the two waste materials were calculated for each experiment from the Cr(VI) content in the solution after ozonation or the advanced oxidation process. This liberation was expressed as a percentage of the total Cr content in the original case study material. All the experiments were repeated at least three times to ensure repeatability. The results reported for each set of unique reaction conditions were the mean obtained from these iterations. Error bars/whiskers indicated on graphs represent the maximum and minimum values obtained experimentally.

3. Results and discussion

3.1. Case study waste material characterisation

The particle size, chemical and surface chemical, and crystalline content characterisation of BFD and the UFS are presented in Tables 1–3, respectively.

In order to quantify the particle size distribution of the BFD and UFS, the d_{90}, d_{50} and d_{10} particle sizes are presented in Table 1. From these results, it is evident that both these materials are too fine for conventional physical separation methods to effectively separate Cr-containing particles from the gauge. In addition, the

Table 1
Particle size analysis of BFD and UFS.

Particle size (μm)	BFD	UFS
D_{90}	29.5	83.1
D_{50}	3.3	14.4
D_{10}	–	0.6

BFD is substantially finer than the UFS, with d_{90} values of 29.5 and 83.1 μm, respectively. The BFD was so fine that the d_{10} could not be determined accurately with the specific instrument utilised.

The chemical compositions of the two case study FeCr waste materials were determined with destructive (ICP–OES, LECO and AAS) and non-destructive (XRF) methods. In general, there is a relatively good correlation between the results of the two different methods (Table 2), although the destructive method is likely to provide more accurate quantitative chemical compositional results. Both these methods indicate that there is still a noteworthy amount of Cr in both these waste materials. Currently, these materials are discarded without any Cr units being recovered. Alumina, magnesium and silicates seem to be the dominant species present apart from the Cr content. This is to be expected, since these species occur in significant fractions in the chromite ore, as well as the fluxes (e.g. quartz, dolomite, magnesite, limestone) utilised in the smelting process. The Cr/Fe ratio of the BFD was 1.42 and for the UFS 1.34. These ratios are a bit lower than that of typical South African metallurgical grade chromite ore of approximately 1.5 and similar to the ratios of the UG2 process residue of approximately 1.4 (Cramer et al., 2004; Howat, 1994). However, these Cr/Fe ratios are not critical in this study since the objective was to liberate only Cr and not Fe. More Na was present in the BFD, which was expected since Na and other volatile metal species are concentrated in particles present in the off-gas of smelters. S was higher in the UFS than the BFD. This is due to the presence of calcium and magnesium in the slag phase during smelting, which results in the formation of calcium sulphide (CaS) and magnesium sulphide (MgS). In fact, all FeCr producers strive to reduce the S content of the FeCr metal. Therefore, the capturing of S in the slag phase is promoted if possible, e.g. basic slag operation that requires the addition of Ca- and/or Mg-containing materials (e.g. dolomite, magnesite, limestone). Surprisingly, the C content of the UFS was relatively high. This could be due to two reasons. Firstly, it is likely that unreacted C-containing reductants (e.g. coke, char and anthracite) are tapped out of the taphole occasionally. This is a relatively common occurrence during periods of metallurgical instability and when the electrode closest to the taphole is short. Secondly, C enrichment in the UFS is likely due to the low density of the carbonaceous particles that will result in these particles mostly reporting to the cyclone overflow during the separation of the ultra-fine slag fraction from the coarser <1 mm slag. Zinc (Zn) was not included in the ICP–OES analysis. However, the XRF analysis clearly indicates the presence of relatively significant concentrations of Zn in both the BFD and UFS. Strobos and Friend (2004) reported a similar level of Zn in another South African FeCr BFD.

The XRD results (Table 3) show the crystalline phase compositions of the materials. The mineral names give the mineral group composition, rather than the actual compositions of the minerals identified. The most significant outcome from these XRD results is the fractional occurrences of chromite in the two case study materials, i.e. 40.1% in BFD and only 8.1% in the UFS. This indicates that the Cr content indicated by the chemical analyses of the BFD originates mostly from unreacted chromite particles. In contrast, the Cr content of the UFS is likely to be a combination of unreacted and/or recrystallised chromite, as well as FeCr particles. Due to limitations of the methods applied FeCr particles was not detected by the XRD analysis. Caution also has to be taken in the comparison of chemical (Table 2) and XRD results (Table 3). XRD only detects the crystalline phases of the sample, within the limitations of the method applied. As an example, the chromite determined with XRD only indicates the crystalline phase materials identified as chromite, and not the concentration of chromite in the overall sample. Thus, the XRD results will not necessarily be consistent with the chemical analysis.

The SEM–EDS results in Table 2 reflect the entire surface area composition of the materials (as defined in Section 2.2). Small amounts of Cr were detected on the surface of both materials, with 2.5% Cr in the BFD and 2.9% in the UFS. The Cr contents determined with chemical analysis (Table 2) were higher than that obtained with SEM–EDS. SEM–EDS could give lower Cr contents for the BFD, since Cr-containing particles could be partially or totally coated by more volatile species condensing on the surface of these particles (Beukes et al., 1999). Therefore, there were larger differences between the SEM–EDS and the chemical analysis results for the Cr content of BFD, than for the UFS. Similar to the chemical analysis, high concentrations of alumina, magnesium and silicates were found in both materials. A Na content of 2.7% was obtained for the BFD, while no Na was observed in the UFS. This also indicates the presence of volatile species condensing on the surface of BFD particles. SEM–EDS also confirmed the higher C and S contents in the UFS, as indicated by the chemical analysis. In general, the surface chemical results corresponded relatively well with the chemical analysis, except for species that could be expected to be concentrated on the surface of particles.

Fig. 1 presents SEM micrographs indicating the general surface characteristics of the two case study materials (Fig. 1a and c) and

Table 2
Chemical and surface chemical characterisation of BFD and UFS.

	BFD	UFS		BFD	UFS
ICP (%)			*LECO C, S and P contents (%)*		
Cr_2O_3	7.66	6.04	C	1.8	14.4
FeO	4.75	3.98	S	1.3	4.2
MgO	23.60	10.30	P2O5 (ppm)	928	999
Al_2O_3	5.85	5.86	*AAS Na contents (%)*		
SiO_2	47.90	42.10	Na	2.4	1.9
CaO	0.66	0.95			
TiO_2	0.16	0.14	*XRF (%)*		
MnO	0.48	0.42	O	–	0.03
ICP (ppm)			MgO	19.70	11.40
As	81	80	Al_2O_3	3.36	5.27
Co	37	35	SiO_2	33.20	36.60
Cu	52	43	P_2O_5	0.01	0.05
Mo	55	59	SO_3	3.61	12.30
Ni	127	103	Cl	0.35	0.11
Pb	520	1460	K_2O	2.07	2.55
V	251	180	CaO	0.40	0.80
Cd	<10	<10	TiO_2	0.14	0.15
SEM–EDS (%)			Cr_2O_3	6.52	5.30
C	4.6	17.2	MnO	0.46	0.424
O	46.9	32.6	Fe_2O_3	4.41	3.86
Na	2.7	–	NiO	0.02	0.02
Mg	13.3	5.6	CuO	–	0.01
Al	2.0	1.9	ZnO	4.20	13.60
Si	18.5	15.6	Ga_2O_3	0.06	0.13
S	1.7	5.2	GeO_2	–	0.01
Cl	0.3	–	Rb_2O	0.02	0.02
K	1.9	2.5	SrO	0.01	0.01
Ca	0.3	0.3	ZrO_2	0.01	0.01
Cr	2.5	2.9	PbO	0.06	0.15
Mn	0.4	0.5	SnO_2	–	0.02
Fe	2.0	2.2	Tl_2O_3	–	0.03
Zn	3.2	13.9			

Table 3
XRD analysis of BFD and UFS.

Crystalline content (%)	BFD	UFS
Chromite	40.1	8.1
Forsterite	52.8	22.9
Magnesioferrite	2.6	19.9
Cristobalite	3.3	
Liebenbergite	1.3	
Wurtzite	–	40.9
Quartz	–	6.6

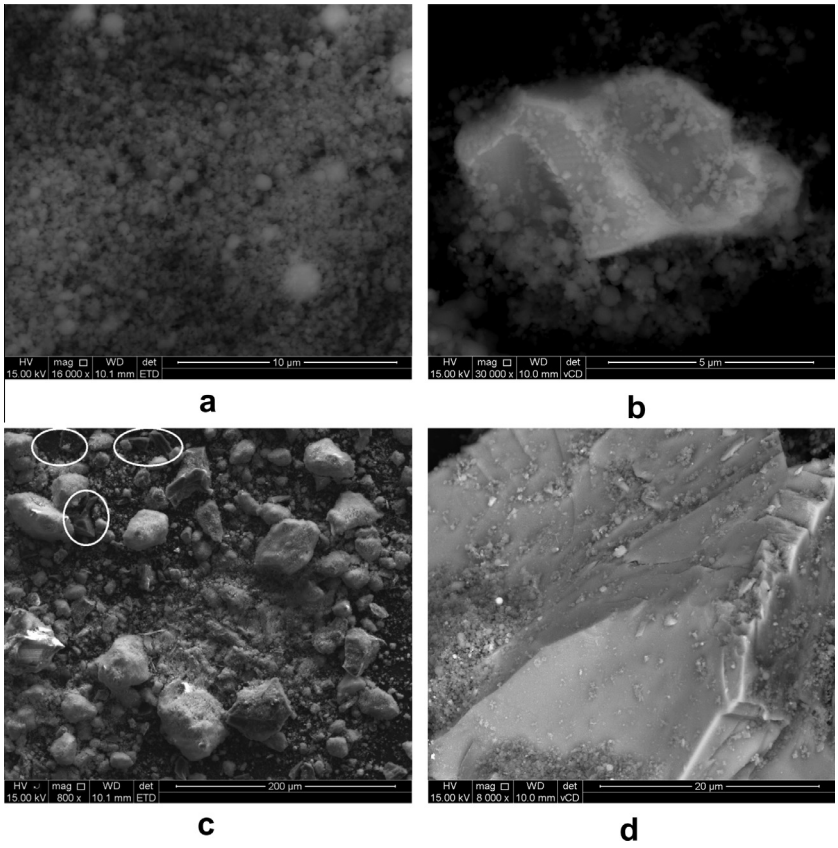

Fig. 1. SEM micrographs of: (a) a BFD sample, (b) an uneven-shaped particle in the BFD, (c) an UFS sample with the white ovals indicating C particles and (d) an uneven-shaped particle in the UFS.

Table 4
SEM-EDS analyses of: (a) the entire surface area of a BFD sample, (b) an unreacted chromite particle in the BFD, (c) the entire area of a UFS sample and (d) an unreacted chromite particle in the UFS.

Analysis number	Cr	Fe	Mg	Al	Si	S	O	Zn	Mn	C	Na	Ti	K	Ca	Cl
a	2.5	2.0	13.3	2.0	18.5	1.7	46.8	3.2	0.4	4.4	2.7	–	1.9	0.3	0.3
b	18.6	13.6	6.4	7.5	3.6	–	45.0	4.3	–	–	–	0.3	0.7	–	–
c	2.9	2.2	5.6	2.0	15.6	5.2	32.6	13.6	0.5	17.2	–	–	2.5	0.3	–
d	26.1	15.3	5.3	5.2	2.6	1.9	33.9	9.4	–	–	–	–	0.3	–	–

specific particles identified in these materials (Fig. 1b and d). In Table 4, the surface chemical composition of the two case study materials and the specific particles indicated in Fig. 1b and d are listed.

It is evident from Fig. 1a that the BFD consisted mostly of very small spherical particles. This micrograph visually confirms the earlier findings (with laser diffraction particle sizing, Table 1) that the BFD particle size distribution is very fine. The spherical shapes of most of the BFD particles suggest that these particles had formed as a result of melting or during condensation. However, the BFD particle matrix did not exclusively consist of spherical particles, since some unevenly shaped particles also occurred. An example of such an uneven-shaped BFD particle is presented in Fig. 1b. SEM–EDS analysis of this particle (Table 4, number b) indicates that it had a significantly higher Cr content than the overall surface analysis (Table 4, number a). This indicates that it is likely to be an unreacted or partially altered chromite particle. In contrast to the BFD matrix that was dominated by spherical-shaped particles, the UFS (Fig. 1c) consisted mostly of uneven-shaped particles. The difference in particle size distribution between the two case study materials is also evident by comparing Fig. 1a with Fig 1c (note the 20 times difference in magnification). C particles, as indicated by the white ovals in the upper left corner of Fig. 1c, are clearly present in the UFS. This agrees with the chemical analysis results, which indicated relatively high C content in UFS. In Fig. 1d, a magnification of a particle within the UFS is presented. SEM-EDS analysis of this particle is shown in Table 4 (number d). The higher Cr content of this particle, i.e. 26.1% Cr, compared to the total UFS matrix surface analysis, i.e. 2.9% Cr, indicates that it is likely to be an unreacted chromite particle. Although not specifically shown in the SEM micrographs presented in Fig. 1, FeCr particles were also present in the UFS.

Considering all the above-mentioned characterisation results of the UFS material, it is evident that its composition differs substantially from conventional FeCr slag. This can be expected, since it was recovered from the overflow of a fine material cyclone at a typical metal recovery plant (Section 2.1). By nature the cyclone overflow material might not be representative of the bulk of the

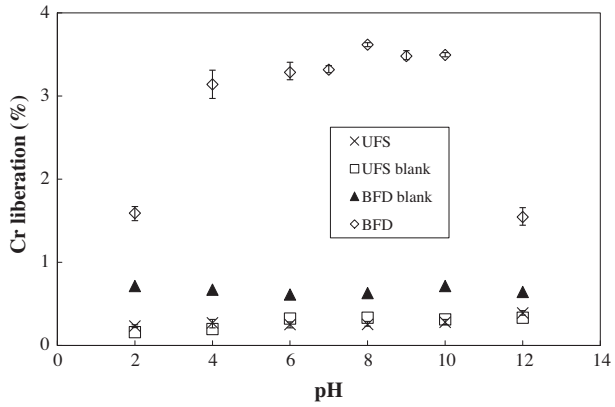

Fig. 2. The effect of aqueous media pH on Cr liberation for both the BFD and UFS. Ozonation contact time = 30 min; solid loading = 2.5 g per 150 ml; gaseous O_3 concentration = 4.5 mg/L; temperature = 24 °C.

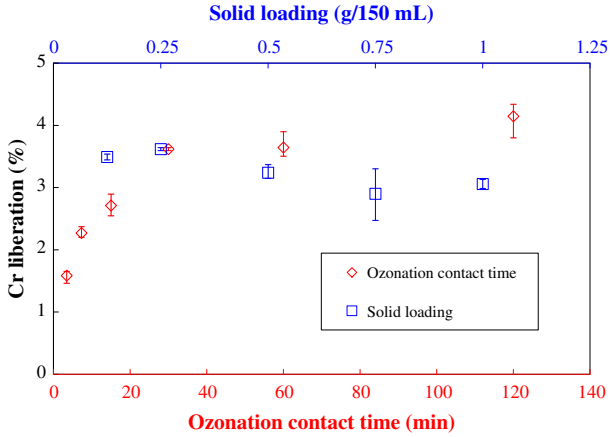

Fig. 3. The effect of ozonation contact time (primary *x*-axis) and solid loading (secondary *x*-axis) on Cr liberation for BFD. pH = 8; ozonation contact time = 30 min (for solid loading only); solid loading = 2.5 g per 150 ml (for ozonation contact time only); gaseous O_3 concentration = 4.5 mg/L; temperature = 24 °C.

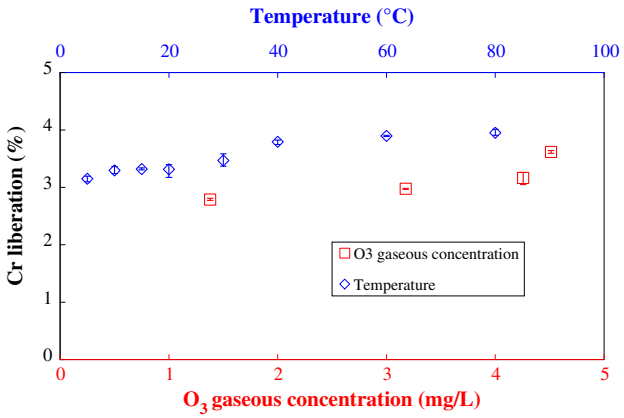

Fig. 4. The effect of O_3 concentration (primary *x*-axis) and temperature (secondary *x*-axis) on Cr liberation for BFD. pH = 8; ozonation contact time = 30 min; solid loading = 2.5 g in 150 ml; gaseous O_3 concentration = 4.5 mg/L (for temperature only); temperature = 24 °C (for O_3 concentration only).

FeCr slag, since it consists of ultra-fine particles and particles with lower density that also reported to the cyclone overflow (e.g. the unusually high C content of the UFS).

3.2. Cr liberation with aqueous ozonation

The Cr(VI) generation with aqueous ozonation that indicated Cr liberation from the waste materials was investigated as a function of pH, ozonation contact time, waste material solid loading, gaseous O_3 concentration and temperature.

3.2.1. pH dependence

Fig. 2 shows the influence of pH on the liberation of Cr(VI) from the two waste materials through the oxidation of Cr(III) and/or Cr(0) to soluble Cr(VI) during aqueous ozonation.

For the BFD, there was a substantial difference in Cr liberation between the blank and ozonation experiments. The Cr liberation from the BFD during ozonation increased with an increase in pH, reaching a maximum at pH 8. Similar levels of Cr liberation were maintained up to pH 10, where after the liberation decreased. The effect of pH on Cr liberation from the BFD during ozonation can be explained by considering previously published data. Ratpukdi et al. (2010) and Lovato et al. (2009) showed that aqueous O_3 is relatively stable at low pH levels, while its spontaneous decomposition to $OH^{\cdot}$ radicals accelerate at higher pH levels. Alhtough aqeous O_3 is a strong oxidant, the $OH^{\cdot}$ radical is a stronger oxidant (Lovato et al., 2009; Von Gunten, 2003; Huang et al., 1993). Therefore, due to higher $OH^{\cdot}$ radical concentrations at elevated pH levels, increased Cr liberation was observed for BFD. However, the increase in Cr liberation associated with increased pH seems to diminish for pH > 10. The exact reason for this observation is currently unclear. However, the extent of Cr liberation from the BFD was not very high, i.e. maximum 3.6%. It is therefore unlikely that this process would be feasible on an industrial scale.

For the UFS there was no meaningful difference in Cr liberation between the blank and ozonation experiments. This implies that neither aqeous O_3 nor its decomposition products, i.e. $OH^{\cdot}$ radicals, were able to liberate Cr from the UFS by oxidation. The differences in the ability of aqueous ozonation to liberate Cr from the two case study materials can be explained by considering their characteristics (Tables 2 and 3). From the chemical and crystalline characteristics of Cr in the two waste materials it is evident that the Cr in the BFD was contained mostly in chromite or partially altered chromite particles, while the Cr in the UFS was contained mostly in FeCr particles. It is therefore feasible to postulate that the Cr(III) present in the chromite and/or partially altered chromite might be more susceptible to oxidation to Cr(VI) than the metallic Cr(0) present in the FeCr. It is well known that Cr(0) enhances the corrosion resistance of materials. Due to the inability of aqueous ozonation to liberate Cr from the UFS, only the liberation of Cr from the BFD was considered in subsequent sections (Section 3.2.2 to 3.2.5), focusing on the effect of other process-controlling parameters.

3.2.2. Ozonation contact time dependence

In order to establish the influence of ozonation contact time on the liberation of Cr, the contact time was varied from 4 to 120 min. The effect of contact time was only investigated at pH 8, since it was the optimum pH for Cr liberation from BFD (Fig. 2). The results presented in Fig. 3 on the primary *x*-axis indicate that longer contact times increase the liberation of Cr. However, after 30 min, the Cr liberation started to stabilise with no significant increases in Cr liberation at longer contact times.

3.2.3. Waste material solid loading dependence

The effect of the amount of BFD solid loading in the aqueous medium at pH 8 (optimal pH) during ozonation is presented in Fig. 3 on the secondary *x*-axis. From these results, it is evident that there was almost a linear relationship with lower solid loading

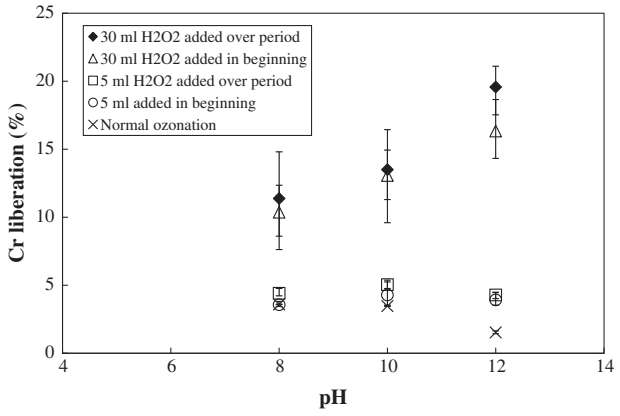

Fig. 5. Cr liberation for BFD with the advanced oxidation process. pH = 8–12; ozonation contact time = 30 min; solid loading = 2.5 g in 150 ml; gaseous O_3 concentration = 4.5 mg/L; temperature = 24 °C.

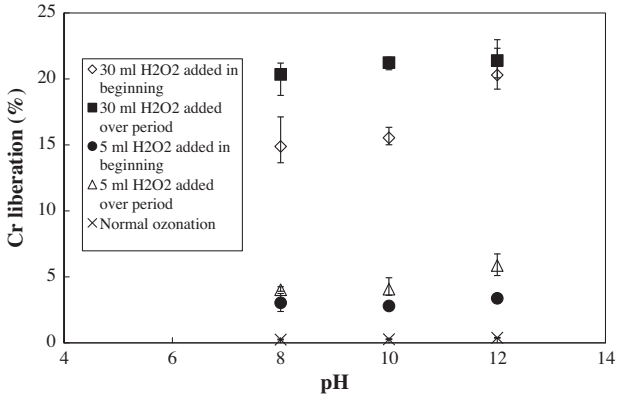

Fig. 6. Cr liberation for UFS with the advanced oxidation process. pH = 8–12; ozonation contact time = 30 min; solid loading = 2.5 g in 150 ml; gaseous O_3 concentration = 4.5 mg/L; temperature = 24 °C.

resulting in higher Cr liberation. This was expected, since higher oxidant concentrations per particle will result in more oxidation.

3.2.4. O_3 concentration dependence

In Fig. 4 on the primary *x*-axis, the effect of O_3 gaseous concentration on Cr liberation at pH 8 (optimum pH) from the BFD is shown. Four different O_3 concentrations were considered. The highest concentration that could be generated by the O_3 generator used was 4.5 mg/L, which was considered to be an experimental limitation. However, notwithstanding the limited O_3 concentration range evaluated, it is evident from the results that Cr liberation increased with increasing gaseous O_3 concentration. The increased O_3 concentration resulted in a higher $OH^{\cdot}$ radical concentration from O_3 decomposition, thereby increasing the amount of Cr liberated through oxidation to Cr(IV).

3.2.5. Temperature dependence

In Fig. 4 on the secondary *x*-axis, the effect of the aqueous ozonation reaction temperature (between 5 and 80 °C) on the liberation of Cr from the BFD at pH 8 (optimum pH) is presented. It can be seen that Cr liberation increases with an increase in temperature. An increase in temperature will lead to an increase in O_3 decomposition (Elovitz et al., 2008; Beltrán, 2003), which will therefore increase the concentration of $OH^{\cdot}$ radicals. As indicated previously, $OH^{\cdot}$ radicals are likely to be the species that are mainly responsible for the oxidation and liberation of Cr in this reaction system.

3.3. Cr liberation with the advanced oxidation process

Since the maximum liberation of Cr with aqueous ozonation was relatively low, i.e. 4.2%, Cr liberation with the advanced oxidation process was also investigated. The advanced oxidation process can be applied in various ways (Bragg et al., 2012; Wu et al., 2004). In this specific study, it was decided to add H_2O_2 during ozonation. According to Rosenfeldt et al. (2006) and Beltrán (2003), the addition of H_2O_2 accelerates the decompostion of aqueous O_3 into $OH^{\cdot}$ radicals. Additionally, the H_2O_2 itself also decomposes to form $OH^{\cdot}$ radicals causing an even higher $OH^{\cdot}$ radical concentration (Bragg et al., 2012; Rodman et al., 2006). If our earlier postulation, i.e. that $OH^{\cdot}$ radicals are mainly responsible for the liberation of Cr through oxidation to Cr(VI), was valid, then the addition of H_2O_2 should enchance Cr liberation.

Since the decomposition of H_2O_2 is favoured at high pH levels (Rosenfeldt et al., 2006), it was decided to perform the advanced oxidation process with H_2O_2 addition during ozonation at pH 8, 10 and 12. H_2O_2 can also serve as a reducing agent for Cr(VI) to Cr(III) at low pH levels (Perez-Benito and Arias, 1997). The liberation of Cr with the advanced oxidation process is presented in Fig. 5 for the BFD and in Fig. 6 for the UFS at the selected pH values. By comparing these results with the liberation results obtained by only utilising aqueous ozonation, it can be stated that Cr liberation was increased significantly. Cr liberation from the BFD was up to five times higher, while up to 20 times higher Cr liberations were achieved from the UFS.

Figs. 5 and 6 illustrate three different process controlling parameters that were tested for each waste material, i.e. the influence of pH, volume H_2O_2 added and method of H_2O_2 addition. From both these figures, three important deductions can be made. Firstly, increased pH resulted in higher Cr liberation. As previously stated, this is related to higher $OH^{\cdot}$ radical concentrations at higher pH levels, which was due to H_2O_2 decomposition (Bragg et al., 2012; Rodman et al., 2006; Rosenfeldt et al., 2006). Secondly, higher volumes of H_2O_2 addition resulted in substantially higher Cr liberation. This was due to higher concentrations of $OH^{\cdot}$ radicals formed as a results of the combined decomposition of O_3 and added H_2O_2 into $OH^{\cdot}$ radicals. Lastly, improved Cr liberation was obtained if H_2O_2 addition was made over the entire contact time, instead of the addition of the total volume at the beginning of the experiment. The latter observation can be attributed to the decomposition of H_2O_2 that occurs relatively fast (Rosenfeldt et al., 2006). In addition, the half-life of the $OH^{\cdot}$ radicals formed is also short (Staehelin and Hoigné, 1982; Rosenfeldt et al., 2006). Therefore, the addition of H_2O_2 over the entire experiment ensured consistently higher $OH^{\cdot}$ radical concentrations in the aqueous medium, which allowed the liberation of more Cr through oxidation.

4. Conclusions

In this paper, two relatively novel procedures to liberate Cr from fine FeCr waste materials were investigated. Limited Cr liberation could be attained from the waste materials by utilising aqueous ozonation to form soluble Cr(VI). For BFD, a maximum of only 4.2% Cr liberation was achieved by studying the influence of several process controlling factors, which included pH, ozonation contact time, waste material solid loading, gaseous O_3 concentration and aqueous media temperature. However, the Cr liberation of BFD was substantially higher than that achieved for the UFS, which was attributed to the difference in characteristics of the two mate-

rials, i.e. the Cr content in BFD was mostly related to chromite and/or altered chromite particles, while the Cr content of the UFS was mostly related to FeCr particles. Comparison of the results presented in this paper with that of Van der Merwe et al. (2012) indicated that Cr liberation from UG2 chromite ore with aqueous ozonation, was much worse than what was achieved for BFD and UFS. It can therefore be concluded that it is more difficult to liberate Cr from unaltered chromite, than from waste materials wherein the Cr occurs in an altered form. The Cr liberation observed was attributed to the formation of $OH^{\cdot}$ radicals during the spontaneous decomposition of aqueous O_3. These radicals are extremely strong oxidising agents.

Although not investigated in such detail, application of the advanced oxidation process by the addition of H_2O_2 during ozonation increased Cr liberation dramatically. 21.1% and 22.3% Cr liberation could be achieved for the BFD and UFS, respectively. The advanced oxidation process provided significantly better results than the aqueous ozonation process, since the addition of H_2O_2 resulted in substantially higher $OH^{\cdot}$ radical concentrations that promoted Cr(VI) formation by oxidation.

Although the above-mentioned levels of Cr-liberation are unlikely to be industrially feasible at present, the investigation proved that further research of especially the advanced oxidation process could optimise Cr-liberation further. During this investigation, O_3 concentrations were limited by the O_3 generator used and only H_2O_2 addition was tested as an example of the advanced oxidation process. The H_2O_2 volume addition was also limited. In future studies, several other peroxide compounds could be considered, while UV radiation and Fe^{2+} addition could also be used to further enhance the process. From the results, it was also evident that the level of Cr liberation depended on the nature of the waste material. Large differences might occur in fine FeCr waste materials between different smelters, due to different smelting technologies (e.g. closed or open/semi-closed SAF, DC arc furnaces, pelletised or ore fed furnaces) and different process control philosophies (e.g. slag basicity) being applied. It is therefore possible that research focusing on a specific fine FeCr waste material, with optimised advanced oxidation process conditions, might result in substantially better Cr liberation. Additional milling of waste materials might also enhance Cr liberation, but that was not considered in this paper. An important future perspective should be to investigate the actual mechanism of Cr liberation by the $OH^{\cdot}$ radical, especially for the advanced oxidation process options. Such mechanistic information would further enable optimisation of the process.

If higher Cr liberation levels can technically be achieved, future research could also consider the techno-economic aspects. The Cr(VI) liberated from the FeCr waste material could be reduced to non-soluble Cr(III) hydroxides in the aqueous media, where after these Cr units could be fed back to the FeCr smelting process. If an aqueous reducing agent other than Fe(II) is used, such Cr(III) hydroxide material could theoretically contain no Fe, which could boost the overall Cr/Fe ratio of the feed material.

In addition, it is well known that the alkaline roasting process to produce Cr(VI) chemicals is not considered to be environmentally friendly and also not ideal from an occupational health perspective. Generating Cr(VI) in aqueous media, as indicated here, could be considered as an alternative in the production of Cr(VI) chemicals, especially since such Cr(VI) compounds could be produced from waste material instead of chromite ore.

Acknowledgements

The authors wish to thank ASA metals for supplying the case study waste materials, Glencore for funding Cr-related research at the North-West University (NWU), as well as the NWU and the NRF for financial support to the M.Sc. studies of Y. van Staden.

References

Andreozzi, R., Caprio, V., Insola, A., 1999. Advance oxidation processes (AOP) for water purification and recovery. Catalysis Today, 51–59.
Beltrán, F.J., 2003. Ozone reaction kinectics for water and wastewater systems. Lewis Publishers, London, pp. 358.
Beukes, J.P., Dawson, N.F., Van Zyl, P.G., 2010. Theoretical and practical aspects of Cr(VI) in the South African ferrochrome industry. The Journal of The Southern African Institute of Mining and Metallurgy 110 (12), 743–750.
Beukes, J.P., Van, P.G., Ras, M., 2012. Treatment of Cr(VI) containing wastes in the South African ferrochrome industry – A review of currently applied methods. The Journal of The Southern African Institute of Mining and Metallurgy 112 (5), 413–418.
Beukes, J.P., Pienaar, J.J., Lachmann, G., Giesekke, E.W., 1999. The reduction of hexavalent chromium by sulphite in wastewater. Water SA 25 (3), 363–370.
Bragg, A., Armstrong, K.C., Xue, Z., 2012. Pretreatment of whole blood usisng hydrogen peroxide and UV irradiation. Design of the advanced oxidation process. Talanta 97, 118–123.
Coetzer, G., Giesekke, E.W., Guest, R.N., 1997. Hexavalent chromium in the recovery of ferrochromium slag. Canadian Metallurgical Quarterly 36 (4), 261–268.
Cortez, S., Teixeira, P., Oliveira, R., Mota, M., 2011. Evaluation of Fenton and ozone-based advanced oxidation processes as mature landfill leachate pre-treatments. Journal of Environmental Management 92, 749–755.
Cramer, L.A., Basson, J., Nelson, L.R., 2004. The impact of platinum production from UG2 ore on ferrochrome production in South Africa. The Journal of The South African Institute of Mining and Metallurgy 104 (9), 517–527.
Dohan, J.M., Masschelein, W.J., 1987. The photochemical generation of ozone: present state-of-the-art. The Journal of the International Ozone association 9 (4), 315–334.
Elovitz, M.S., Von Gunten, U., Kaiser, H., 2008. Hydroxyl radical/ozone ratios during ozonation processes II. The effect of temperature, pH, alkalinity and DOM properties. Ozone: Science and Engineering. The Journal of International Ozone Association 22 (2), 123–150.
Gericke, W.A., 1995. Environmental aspects of ferrochrome production. Proceedings Ferroalloys 7th international congress (INFACON XII). Trondheim, Norway, pp. 131–140.
Howat, D.D., 1994. Chromium in South Africa. The Journal of the South African Institute of Mining and Metallurgy 86 (2), 37–50.
Huang, C.P., Dong, C., Tang, Z., 1993. Advanced chemical oxidation: Its present role and potential future in hazardous waste treatment. Waste Management 13 (5–7), 361–377.
IARC (International Agency for Research on Cancer). 1997. World Health 0rganisation . IARC monographs on the evaluation of carcinogenic risks to humans, Chromium, Nickel and Welding, vol. 49.
ICDA (International Chomium Development Association). 2010. Statistical Bulletin 2010 eition. Paris, France.
ISSF: International stainless steel forum. 2011. Stainless steel demand index. <http://www.worldstainless.org/Statistics/Demand+index/>. (accessd: 20.01.2012).
Lovato, M.E., Martín, A.M., Cassano, A.E., 2009. A reaction kinetic model for ozone decomposition in aqueous media valid for the neutral and acidic pH. Chemical Engineering Journal 146, 486–497.
McElroy, F., Mikel, D. and Nees, M. 1997. Determination of ozone by ultraviolet analysis, A New Method for Volume II, Ambient Air Specific Methods, Quality Assurance Handbook for Air Pollution Measurement Systems. <http://mattson.creighton.edu/Ozone/OzoneEPAMethod.pdf>. (accessed : 19.09.2012).
Murthy, Y.R., Tripathy, S.K., Kumar, C.R., 2011. Chrome ore beneficiation challenges & opportunities – a review. Minerals Engineering 24, 375–380.
Naiker, O. Riley, T. 2006. Xstrata Alloys in Profile. In: Southern African Pyrometallurgy 2006 Conference, Johannesburg, South African Institute of Mining and Metallurgy. pp. 297-306.
Neyens, E., Bayens, J., 2003. A review of classic Fenton's peroxidation as an advanced oxidation technique. Journal of Hazardous Materials B98, 33–50.
Perez-Benito, J.F., Arias, C., 1997. A Kinetic Study of the Chromium(VI)-Hydrogen Peroxide Reaction. Role of the Diperoxochromate(VI) Intermediates. Journal of Physical Chemistry A 101, 4726–4733.
Rao, D.S., 2010. Valuble waste. Recovery of chromite values from ferrochrome industry flue dust. <http://www.at-online.info/download/215793/12_Research_Development.pdf>. (accessed: 25.07.2013).
Ratpukdi, T., Siripattankul, S., Khan, E., 2010. Mineralization and biodegradability enhancement of natural organic matter by ozone –VUV in comparison with ozone, VUV, ozone-UV, and UV: Effects of pH and ozone dose. Water Research 44, 3531–3543.
Riekkola-Vanhanen, M., 1999. Finnish expert report on best available techniques in ferrochromium production. Helsinki.
Rodman, D.L., Carrington, N.A., Xue, Z., 2006. Conversion of chromium(III) propionate to chromium(VI) by the advanced Oxidation Process. Pretreatment of a biomimetic complex for metal analysis. Talanta 70, 668–675.
Rosenfeldt, E.J., Linden, K.G., Canonica, S., Von Gunten, U., 2006. Comparison of the efficiency of $^{\bullet}OH$ radical formation during ozonation and the advanced oxidation processes O_3/H_2O_2 and UV/H_2O_2. Water Research 40, 3695–3704.
Sripriya, R., Murty, V.G.K., 2004. Recovery of metal from slag/mixed metal generated in ferroalloys plants-a case study. International Journal of Mineral Processing 75, 123–134.

Shen, H., Forssberg, E., 2002. An overview of recovery of metals from slags. Waste Management 23, 933–949.
Staehelin and Hoigné, J., 1982. Decomposition of ozone in water: Rate of initiation by hydroxide ions and hydrogen peroxide. Environmental Science and Technology 16 (10), 676–681.
Strobos, J.G., Friend, J.F.C., 2004. Zinc recovery from baghouse dust generated at ferrochrome foundries. Hydrometallurgy 74, 165–171.
Van der Merwe, W., Beukes, J.P., Van Zyl, P.G., 2012. Cr(VI) formation during ozonation of Cr-containing materials in aqueous suspension – implications for water treatment. Water SA 38 (4), 505–510.
Visser, J., Barret, W., 1992. An evaluation of process alternatives for the reclamation of ferrochrome slag. *Proceedings Ferroalloys 6th international congress* (INFACON VI). Cape Town, South. Africa, 107–112.
Vogel, A.I. 1978. Vogel's Textbook of quantitative inorganic analysis, including elementary instrumental analysis. Revised by Basset, J., Denney, R.C., Jeffery, G.H., Mendham, J. London: Longman. pp. 362–363.
Von Gunten, U., 2003. Ozonation of drinking water: Part I. Oxidation kinetics and product formation. Water research 37, 1443–1467.
Wu, J.J., Wu, C., Ma, H., Chang, C., 2004. Treatment of landfill leachate by ozone-based advanced oxidation processes. Chemosphere 54, 997–1003.